

1 **Uncovering the hidden antibiotic potential of Cannabis**

2

3

4 Maya A. Farha^{1,2, †}, Omar M. El-Halfawy^{1,2,3, †}; Robert T. Gale^{1,2}; Craig R. MacNair^{1,2}; Lindsey A.
5 Carfrae^{1,2}; Xiong Zhang^{1,2}, Nicholas G. Jentsch^{1,2}; Jakob Magolan^{1,2}; Eric D. Brown^{1,2*}

6

7 ¹ Department of Biochemistry and Biomedical Sciences, McMaster University, Hamilton, Ontario L8N
8 3Z5, Canada

9 ² Michael G. DeGrootte Institute of Infectious Disease Research, McMaster University, Hamilton,
10 Ontario, L8N 3Z5, Canada

11 ³ Microbiology and Immunology Department, Faculty of Pharmacy, Alexandria University,
12 Alexandria, 21521, Egypt

13 * To whom correspondence should be addressed (ebrown@mcmaster.ca)

14 † These authors contributed equally

15

16

17

18

19

20

21

22

23

24

25 **Abstract**

26

27 The spread of antimicrobial resistance continues to be a priority health concern worldwide,
28 necessitating exploration of alternative therapies. *Cannabis sativa* has long been known to contain
29 antibacterial cannabinoids, but their potential to address antibiotic resistance has only been
30 superficially investigated. Here, we show that cannabinoids exhibit antibacterial activity against
31 MRSA, inhibit its ability to form biofilms and eradicate pre-formed biofilms and stationary phase cells
32 persistent to antibiotics. We show that the mechanism of action of cannabigerol is through targeting the
33 cytoplasmic membrane of Gram-positive bacteria and demonstrate *in vivo* efficacy of cannabigerol in a
34 murine systemic infection model caused by MRSA. We also show that cannabinoids are effective
35 against Gram-negative organisms whose outer membrane is permeabilized, where cannabigerol acts on
36 the inner membrane. Finally, we demonstrate that cannabinoids work in combination with polymyxin B
37 against multi-drug resistant Gram-negative pathogens, revealing the broad-spectrum therapeutic
38 potential for cannabinoids.

39

40

41

42

43

44

45

46

47

48

49

50

51

52

53

54

55

56

57

58

59

60

61

62 Public Health agencies around the globe have identified antimicrobial resistance as one of the
63 most critical challenges of our time. The rapid and global spread of antimicrobial-resistant organisms in
64 recent years has been unprecedented. So much so that the world health organization (WHO) published
65 its first ever list of antibiotic-resistant "priority pathogens", made up of 12 families of bacteria that pose
66 the greatest threat to human health¹. Among them, *Staphylococcus aureus* is the leading cause of both
67 healthcare and community-associated infections worldwide and a major cause for morbidity and
68 mortality², especially with the emergence and rapid spread of methicillin-resistant *S. aureus* (MRSA),
69 which is resistant to all known β -lactam antibiotics³. Worse yet, resistance to vancomycin, linezolid
70 and daptomycin has already been reported in MRSA clinical strains, compromising the therapeutic
71 alternatives for life-threatening MRSA infections⁴. Further, antibiotic-resistant Gram-negative
72 infections have increasingly become a pressing issue in the clinic. Indeed, of the bacteria highlighted
73 by the WHO, 75% are Gram-negative organisms. Among the currently approved antibiotics in clinical
74 use, the latest discovery of a new drug class dates back to more than 30 years ago. The rapid loss of
75 antibiotic effectiveness and diminishing pipeline beg for the exploration of alternative therapies.

76 *Cannabis* plants are important herbaceous species that have been used in folk medicine for
77 centuries. Increasing scientific evidence is accumulating for the efficacy of its metabolites in the
78 treatment, for example, of epilepsy, Parkinson disease, analgesia, multiple sclerosis, Tourette's
79 syndrome and other neurological diseases⁵. At a very nascent stage are investigations into the potential
80 of cannabis metabolites as antibacterial therapies. To date, assessments of their antibacterial activity
81 have been few and superficial. *In vitro* studies have shown that cannabinoids inhibit the growth of
82 Gram-positive bacteria, mostly *S. aureus*, with no detectable activity against Gram-negative
83 organisms⁶⁻⁹, where the clinical need is highest. Further, the mechanism of action has remained elusive
84 and there has been little validation of antibacterial activity *in vivo*.

85 Here, we show that cannabinoids exhibit antibacterial activity against MRSA, inhibit its ability
86 to form biofilms, eradicate pre-formed biofilms and stationary phase cells persistent to antibiotics. We
87 reveal that the mechanism of action of cannabigerol (CBG) is through targeting the cytoplasmic
88 membrane of Gram-positive bacteria and demonstrate *in vivo* efficacy of CBG in a murine systemic
89 infection model caused by MRSA. We also show that cannabinoids are effective against Gram-negative
90 organisms whose outer membrane is permeabilized, where CBG acts on the inner membrane. Finally,
91 we demonstrate that cannabinoids work in combination with polymyxin B against multi-drug resistant
92 Gram-negative pathogens, revealing the broad-spectrum therapeutic potential for cannabinoids. In all,

93 our findings position cannabinoids as promising leads for antibacterial development that warrant
94 further study and optimization.

95

96 **Results and Discussion**

97

98 We began our study investigating the antibacterial, anti-biofilm and anti-persister activity of a
99 variety of commercially available cannabinoids, including the five major cannabinoids,
100 cannabichromene (CBC), cannabidiol (CBD), cannabigerol (CBG), cannabinol (CBN), and Δ^9 -
101 tetrahydrocannabinol (THC), as well as a selection of their carboxylic precursors (pre-cannabinoids)
102 and other synthetic isomers (18 unique molecules total, Fig. 1) against methicillin-resistant *S. aureus*
103 (MRSA) (Supplementary Table 1). Susceptibility tests were conducted according to the Clinical and
104 Laboratory Standards Institute (CLSI) protocol against MRSA USA300, a highly virulent and prevalent
105 community-associated MRSA. Overall, antibacterial activities for the five major cannabinoids (and
106 some of their synthetic derivatives) were in line with previously published work⁶⁻⁸. Seven molecules
107 were potent antibiotics with minimum inhibitory concentration (MIC) values of 2 $\mu\text{g/mL}$, including
108 CBG, CBD, CBN, cannabichromenic acid (CBCA) and THC along with its Δ^8 - and exo-olefin
109 regioisomers. We observed moderate loss of potency associated with the benzoic acid moiety (CBG,
110 CBD, and THC were more potent than CBGA, CBDA, THCA) and when n-pentyl substituent was
111 replaced with n-propyl (CBD and THC were superior to CBDV and THCV) (Supplementary Table 1).
112 These two modifications appeared to have an additive detrimental effect on antibacterial activity
113 (THCVA, CBDVA). The two most common human metabolites of THC, (\pm) 11-nor-9-carboxy- Δ^9 -
114 THC, and (\pm) 11-hydroxy- Δ^9 -THC, as well as cannabicylol were inactive at the highest concentrations
115 screened (MIC > 32 $\mu\text{g/mL}$) (Supplementary Table 1).

116 Biofilm formation by MRSA, typically on necrotic tissues and medical devices, is considered
117 an important virulence factor influencing its persistence in both the environment and the host
118 organism¹⁰. These highly structured surface-associated communities of MRSA are typically associated
119 with increased resistance to antimicrobial compounds and are generally less susceptible to host immune
120 factors. We assessed the ability of the various cannabinoids to inhibit the formation of biofilms by
121 MRSA, using static abiotic solid-surface assays in which MRSA was treated with increasing
122 concentrations of cannabinoids under conditions favouring biofilm formation (Supplementary Fig. 1).
123 In all, the degree of inhibition of biofilm formation correlated with antibacterial activity; those
124 cannabinoids with potent activity against MRSA strongly suppressed biofilm formation and vice versa
125 (Supplementary Fig. 1, Supplementary Table 1). The five major cannabinoids clearly repressed MRSA
126 biofilm formation, with CBG (Fig. 2a) exhibiting the most potent anti-biofilm activity. Indeed, as little

127 as 0.5 µg/mL (1/4 MIC) of CBG inhibited biofilm formation by ~50% (Fig. 2b). Thus, this experiment
128 underlined the strong inhibitory effect of cannabinoids on biofilm formation; this sub-MIC level of
129 CBG did not affect planktonic growth (Supplementary Fig. 2). Interestingly, we also evaluated the
130 effect of CBG on pre-formed biofilms by determining its minimal biofilm eradication concentration
131 (MBEC); CBG could eradicate pre-formed biofilms of MRSA USA300 at 4 µg/mL (Fig. 2c).

132
133 Another challenge in the treatment of MRSA infections is the formation of non-growing,
134 dormant ‘persister’ subpopulations that exhibit high levels of tolerance to antibiotics¹¹⁻¹³. Persister cells
135 have a role in chronic and relapsing *S. aureus* infections¹⁴ such as osteomyelitis¹⁵, and endocarditis¹⁶.
136 Here, we evaluated the killing activity of a series of cannabinoids against persisters derived from
137 stationary phase cells of MRSA USA300 (Supplementary Fig. 3). These have been previously shown to
138 be tolerant to conventional antibiotics such as gentamicin, ciprofloxacin and vancomycin^{11, 17-18}. In
139 general, the anti-persister activity correlated with potency against actively dividing cells as determined
140 by MIC assays (Supplementary Table 1). Again, CBG was the most potent cannabinoid against
141 persisters, whereas oxacillin and vancomycin were ineffective at concentrations that otherwise kill
142 actively dividing cells (Supplementary Fig. 3, Fig. 2d). More specifically, CBG killed persisters in a
143 concentration-dependent manner starting at 5 µg/ml. Notably, CBG rapidly eradicated a population of
144 ~10⁸ CFU/ml MRSA persisters to below the detection threshold within 30 minutes of treatment (Fig.
145 2d).

146 We selected CBG (Fig.2a) for further studies of mechanism and *in vivo* efficacy. Not only did
147 CBG potently inhibit MRSA (MIC 2 µg/mL), repress biofilm formation (Fig. 2b), eradicate pre-formed
148 biofilms (Fig. 2c) and effectively eradicate persister cells (Fig. 2d), but it is non-psychotropic, non-
149 sedative and constitutes a component of *Cannabis* for which there is high therapeutic interest¹⁹. While
150 it has many desirable pharmacological properties, CBG also possesses several desirable physico-
151 chemical properties as a medicinal chemistry lead in terms of molecular weight, number of hydrogen
152 donors and acceptors, number of rings and rotatable bonds (Table 1). Nevertheless, CBG suffers from
153 high lipophilicity (high log P) and low aqueous solubility (Table 1). These values were not a bottleneck
154 to our studies, but in moving CBG as a lead, such properties could be addressed in medicinal chemistry
155 campaigns. To our advantage, we were able to synthesize CBG efficiently from olivetol and geraniol,
156 two inexpensive precursors, in one synthetic operation. We were cognisant that such facile synthetic
157 access would enhance the potential for subsequent medicinal chemistry-based development efforts.
158 We determined the MIC₉₀ of CBG against 96 clinical isolates of MRSA using the CLSI protocol. The
159 corresponding frequency distribution of MICs is presented in Fig. 2e. The MICs ranged from 2 – 8

160 $\mu\text{g/mL}$ with a resulting MIC_{90} of $4 \mu\text{g/mL}$. The range of MIC values was tight with only one outlier
161 strain detected to have a very low MIC of 0.0625. Overall, this activity compares favourably with
162 conventional antibiotics for these multi-drug resistant strains.

163 Given its growth inhibitory action on Gram-positive bacteria, we reasoned isolating resistant
164 mutants to CBG would be a straightforward approach to gather insights into its bacterial target. Indeed,
165 resistance mutations can often be mapped to a drug's molecular target²⁰. To this end, MRSA was
166 repeatedly challenged with various lethal concentrations of CBG, ranging from 2-16x MIC, to select
167 for spontaneous resistance in MRSA (Fig. 3). No spontaneously resistant mutants were obtained,
168 indicating a frequency of resistance less than 10^{-10} for MRSA. We also attempted to allow MRSA
169 bacteria to develop resistance to CBG by sequential subcultures via 15-day serial passage in liquid
170 culture containing sub-MIC concentrations of CBG and, again, no change in the MIC of CBG was
171 detected (Fig. 3). While these experiments were unsuccessful probes of mechanism, they suggested
172 very low rates of resistance for CBG, a highly desirable property for an antibiotic.

173 We turned to chemical genomic analysis to generate hypotheses for the target of CBG. Such
174 studies can reveal patterns of sensitivity among genetic loci that are characteristic of the mechanism of
175 action of an antibacterial compound²¹. We confirmed that the model Gram-positive bacterium *B.*
176 *subtilis* was susceptible to CBG (MIC $2 \mu\text{g/mL}$), and screened a CRISPR interference knockdown
177 library of all essential genes in *B. subtilis*²² for further sensitization to CBG. In the absence of
178 induction, relying on basal repression (which leads to a ~3-fold repression of the knockdown library²²),
179 we were unable to detect any knockdowns sensitized to sub-lethal concentrations of CBG (Fig. 3).
180 Low-level induction identified some sensitive and some suppressing clones, however follow-on work
181 with the individual knockdowns in liquid culture via full checkerboard analysis (combining xylose, the
182 inducer, with CBG) failed to confirm sensitivity or suppression. In all, we were unable to identify *bona*
183 *fide* chemical genetic interactions among essential genes of *B. subtilis* and CBG. We next aimed to
184 query the non-essential gene subset, this time using the Nebraska Transposon Mutant Library, a
185 sequence-defined transposon mutant library consisting of 1,920 strains, each containing a single
186 mutation within a nonessential gene of CA-MRSA USA300²³, again looking for genetic enhancers or
187 suppressors to generate target hypotheses (Fig. 3, Supplementary Fig. 4a). While we were unable to
188 uncover genetic suppressors at supra-lethal concentrations of CBG, we identified 41 transposons as
189 sensitive across 3 different sub-lethal concentrations of CBG (Supplementary Table 2). Analysis of
190 these transposons revealed a significant enrichment for genes encoding proteins that are localized at the
191 cytoplasmic membrane (Supplementary Fig. 4b) and enrichment for genes encoding functions in
192 processes that take place at the cytoplasmic membrane, such as cellular respiration and electron

193 transport chain (Supplementary Fig. 4c). In all, chemical genomic profiling with CBG generally linked
194 its activity to cytoplasmic membrane function.

195 The lack of clear targets among the essential gene products, the predominance of chemical
196 genetic interactions linked to membrane function, and the difficulty generating resistant mutants,
197 suggested that CBG might act on the cytoplasmic membrane of MRSA. Indeed, the propensity of
198 membrane-active compounds to generate resistance is frequently low²⁴. Further, the bacterial
199 membrane is critical for cell function and survival, and is essential irrespective of the metabolic status
200 of the cell, including non-growing and persisting cells²⁴. The strong action of CBG on persister cells
201 would be consistent with such a mode of action. Thus, we assessed the ability of CBG to disrupt
202 membrane function using the membrane potential-sensitive probe, 3,3'-dipropylthiadicarbocyanine
203 iodide (DiSC₃(5)). In DiSC₃-loaded MRSA cells, CBG caused a dose-dependent increase in
204 fluorescence that occurred at a concentration consistent with the MIC of CBG (Fig. 3). To probe the
205 possibility that CBG selectively dissipated membrane potential ($\Delta\psi$) component of proton motive
206 force, we tested for synergy with sodium bicarbonate, a known perturbant of ΔpH , that has been shown
207 to synergize with molecules that reduce $\Delta\psi$ ²⁵. A lack of synergy between these compounds suggested
208 CBG disrupts the integrity of the cytoplasmic membrane (Supplementary Fig. 5). In order to evaluate
209 the potential membrane activity of CBG on mammalian cells, we evaluated its hemolytic toxicity
210 across varying concentrations (Supplementary Fig. 6). CBG was hemolytic only at 32 $\mu\text{g/mL}$, above its
211 MIC of 2 $\mu\text{g/mL}$, suggesting some specificity for prokaryotic cells.

212 Having established strong *in vitro* potency for CBG against MRSA, we next sought to evaluate
213 the *in vivo* efficacy in a murine systemic infection model of MRSA. The effect of CBG on a systemic
214 infection mediated by the CA-MRSA USA300 strain is shown in Fig. 4. A dose-dependence study
215 (Supplementary Fig. 7) informed that a dose of 100 mg/kg is most effective while remaining tolerable.
216 To evaluate tolerability, we treated mice with 100 mg/kg CBG and assessed their change in body
217 weight over various time points and found no significant changes (Supplementary Fig. 8). Additionally,
218 no signs of acute toxicity have been reported in a pharmacokinetic study of 120-mg/kg doses of
219 CBG²⁶. Overall, CBG displayed a significant reduction in bacterial burden in the spleen by a factor of
220 2.8- \log_{10} in CFU compared to the bacterial titer seen with the vehicle ($p < 0.001$, Mann-Whitney *U*-
221 test). Further, the *in vivo* efficacy of CBG was comparable to that of the antibiotic control, vancomycin
222 administered at a similar dose. In all, CBG displayed promising levels of efficacy in the systemic
223 infection model.

224 To date, antibacterial activity of cannabinoids against Gram-negative organisms has largely
225 been ruled out, since reported MICs values fall in the 100-200 $\mu\text{g/mL}$ range⁷⁻⁸. We confirmed this,

226 obtaining MICs $>128 \mu\text{g/mL}$ for all of the tested cannabinoids against the model Gram-negative
227 organism *Escherichia coli*. Given the observed action of CBG on the cytoplasmic membrane of MRSA,
228 we reasoned that CBG (and other cannabinoids) might be equally effective on the Gram-negative
229 counterpart, the inner membrane. Further, just as many antibacterial compounds fail to work against
230 Gram-negative pathogens due to a permeability barrier²⁷, we reasoned that low permeability across the
231 outer membrane (OM) may be the reason for the poor efficacy of cannabinoids. Thus, we investigated
232 the antibacterial profile of the five major cannabinoids against *E. coli*, where their permeation was
233 facilitated through the OM by means of chemical perturbation. To this end, we set up checkerboard
234 assays to assess the interaction of CBG (Fig. 5a) and the four other main cannabinoids (Supplementary
235 Fig. 9) with the membrane perturbant, polymyxin B against *E. coli*. Remarkably, all five major
236 cannabinoids gained potent activity in the presence of sub-lethal concentrations of polymyxin B.
237 Indeed, all interactions were deemed synergistic (Fig. 5, Supplementary Fig. 9). For example, CBG,
238 which was inactive against *E. coli* ($>128 \mu\text{g/mL}$), was strongly potentiated when combined with a sub-
239 lethal concentration of polymyxin B ($1 \mu\text{g/mL}$ in the presence of $0.062 \mu\text{g/mL}$ polymyxin B). A similar
240 synergistic interaction was observed with polymyxin B nonapeptide, a less toxic derivative of
241 polymyxin B that strictly perturbs the outer membrane in Gram-negative bacteria (Supplementary Fig.
242 10), suggesting that induction of outer membrane permeability is sufficient to allow entry and activity
243 of CBG. We further assessed whether OM perturbation by genetic means would lead to similar results
244 by evaluating the activity of CBG against a number of strains where the OM was compromised (Fig.
245 5b). In an *E. coli* $\Delta\text{bamB}\Delta\text{tolC}$ deletion strain, which renders *E. coli* hyperpermeable to many small
246 molecules, due to loss of BamB, a component of the β -barrel assembly machinery for OM proteins and
247 TolC, the efflux channel in the outer membrane, CBG had a MIC of $4 \mu\text{g/mL}$, on par with its Gram-
248 positive activity. Similarly, in a hyperporinated, $\Delta 9$ strain of *E. coli*, where a recombinant pore was
249 introduced in the OM and all nine known TolC-dependent transporters deleted²⁸, CBG activity became
250 evident with a MIC of $8 \mu\text{g/mL}$. Finally, in an *Acinetobacter baumannii* deficient in
251 lipooligosaccharide (LOS-), which effectively alters the permeability of the OM²⁹, CBG activity was
252 enhanced greater than 128-fold, resulting in a MIC value of $0.5 \mu\text{g/mL}$. Overall, these results suggest
253 that cannabinoids face a permeability barrier in Gram-negative bacteria and further imply that
254 cannabinoids inhibit a bacterial process present in Gram-negative pathogens, and likely common to that
255 in Gram-positive pathogens.

256 To this end, we investigated whether CBG acted on the inner membrane (IM) of *E. coli* as well
257 as the OM. IM and OM permeability were determined, respectively, from ortho-Nitrophenyl- β -
258 galactoside (ONPG) and nitrocefin hydrolysis in an *E. coli* strain constitutively expressing a

259 cytoplasmic β -galactosidase and a periplasmic β -lactamase while lacking the lactose permease, as
260 described in the literature³⁰. As shown in Fig. 5c, CBG specifically acted on the IM, and only in the
261 presence of polymyxin B at a sub-lethal concentration that had minimal effects on the IM alone. We
262 observed that CBG (+polymyxin B) induced major permeability changes in the inner membrane,
263 indicated by a time-dependent marked increase in optical density values due to ONPG hydrolysis as a
264 result of unmasking the cytoplasmic β -galactosidase, which can only occur with destabilization of IM
265 (Fig. 5c). CBG exhibited no action on the OM (Supplementary Fig. 11). Overall, the mechanism of
266 bacterial killing by CBG in *E. coli* is likely loss of IM integrity and requires antecedent OM
267 permeabilization.

268 Combination antibiotic therapy is becoming an increasingly attractive approach to combat
269 resistance³¹. So too is the strategy of using an OM perturbing molecule to facilitate the permeation of
270 compounds that are otherwise active only on Gram-positive bacteria³². We assessed the therapeutic
271 potential of the adjuvant polymyxin B in combination with CBG to inhibit the growth of priority Gram-
272 negative pathogens such as *A. baumannii*, *E. coli*, *Klebsiella pneumoniae*, and *Pseudomonas*
273 *aeruginosa* (Fig. 5d). We employed conventional checkerboard assays to determine the interaction and
274 potency of CBG and polymyxin B when used concurrently against various multi-drug resistant clinical
275 isolates. In all cases, synergy was evident, suggesting the potential for combination therapy of the
276 cannabinoids with polymyxin B against Gram-negative bacteria.

277 In summary, we have investigated the therapeutic potential of cannabinoids, specifically CBG,
278 through a comprehensive study of *in vitro* potency on biofilms and persisters, as well as mechanism of
279 action studies and *in vivo* efficacy experiments. Most notably, we have uncovered the hidden broad-
280 spectrum antibacterial activity of cannabinoids and demonstrated the potential of CBG against Gram-
281 negative priority pathogens. Taken together, our findings lend credence to the idea that cannabinoids
282 may be produced by *Cannabis sativa* as a natural defense against plant pathogens. Notwithstanding,
283 cannabinoids are well-established as drug compounds that have favourable pharmacological properties
284 in humans. The work presented here suggests that the cannabinoid chemotype represents an attractive
285 lead for new antibiotic drugs.

286
287 **Acknowledgements** This work was supported by a salary award to E.D.B from the Canada Research
288 Chairs program and operating funds to E.D.B from a CIHR Foundation grant (FDN-143215); by
289 a Michael G. DeGroote Centre for Medicinal Cannabis Research post-doctoral fellowship to O.M.E.
290 Synthetic chemistry was supported by McMaster's Faculty of Health Sciences and the Michael G.
291 DeGroote Institute for Infectious Disease Research. We thank Shawn French for preparing the
292 graphical abstract.

293 **Author contributions** M.A.F., O.M.E., R.T.G., and E.D.B. conceived and designed the research.
294 M.A.F. and O.M.E., performed all experiments and analyzed data with the exception of the mouse
295 infection model and the synthesis of CBG. C.R.M. and L.A.C. performed the mouse infection model.
296 X.Z. and N.G.J. optimized a scalable synthesis of CBG, supervised by J.M. M.A.F. and E.D.B. wrote
297 the paper, with large input from O.M.E. All authors approved the final version.

298 **Competing interests** E.D.B., J.M., M.A.F., O.M.E., and R.T.G. are inventors on a patent application
299 on the use of cannabinoids for prevention and/or treatment of infections.

300 METHODS

301 **Strains and reagents.** Supplemental Table 3 lists bacteria and plasmids used in this work. Supporting
302 Information *S. aureus* Table lists the 96 clinical isolates, along with body site location and year of
303 isolation. Bacteria were grown in cation-adjusted Mueller Hinton broth (CAMHB) at 37°C, unless
304 otherwise stated. Antibiotics were obtained from Sigma, Oakville, ON, Canada. Pure cannabinoid
305 solutions purchased from Sigma, Oakville, ON, Canada were used for all experiments. Only CBG was
306 synthesized in larger quantity as described below.

307 **Antimicrobial susceptibility testing.** Minimum inhibitory concentration (MIC) determination and
308 checkerboard assays were conducted following the guidelines of CLSI for MIC testing by broth
309 microdilution³³. Persister killing activity of cannabinoids was evaluated against stationary-phase cells
310 of *S. aureus* as previously described³⁵.

311 ***B. subtilis* CRISPRi essential gene knockdown strain collection screen.** Overnight cultures of the
312 collection²² (at a 96-well density, $n = 289$) were performed using the Singer rotor HDA (Singer
313 Instruments, United Kingdom) in CAMHB. Subsequently, CAMHB with or without CBG were
314 inoculated using the singer rotor at 96-well density. These experiments were performed either in the
315 presence of 0.05% xylose (allowing low level of *dcas9* expression) or with no xylose induction
316 (basal *dcas9* expression). The plates were incubated at 37°C and OD₆₀₀ was read after 24 h.

317 ***S. aureus* Nebraska Transposon Mutant Library (NTML) screen.** Overnight cultures of the
318 NTML²³ (at a 384-well density) were performed using the Singer rotor HDA (Singer Instruments,
319 United Kingdom) in CAMHB containing erythromycin (5 µg/mL). Subsequently, CAMHB with or
320 without CBG were inoculated using the singer rotor at 384-well density. The plates were incubated at
321 37°C and OD₆₀₀ was read after 24 h. Cellular localization and functional (gene ontology, GO-term)
322 enrichment analyses were performed using Pathway Tools software and MetaCyc database³⁶.

323 **Selection of suppressor mutants of CBG activity in *S. aureus*.** Spontaneous suppressor mutants were
324 selected for in liquid culture. Briefly, isolated colonies were resuspended in PBS and diluted to a final
325 OD₆₀₀ of 0.05 into 200 µL of CAMHB containing CBG (at 4x and 8x MIC) set up in 96-well microtiter
326 plates, 36 wells/concentration. Plates were incubated at 37°C for 4 days. Alternatively, bacteria were
327 treated with a 2-fold series of CBG concentrations spanning the MIC. Bacteria growing at the
328 maximum sub-MIC concentration were repeatedly passaged in a similar series of CBG concentrations
329 by 1000-fold dilution every 24 hours. Five CBG dilution series were performed simultaneously and the
330 cells were passaged for 15 days.

331 **General molecular techniques.** DNA manipulations were performed as previously described³⁷. CaCl₂
332 chemically-competent ML35 cells were transformed with pBR322 encoding a periplasmic β-lactamase.

333 **Biofilm formation assays.** Biofilm formation was performed in polystyrene 96-well plates in Tryptic
334 Soy Broth (TSB) with 1% glucose and detected by the crystal violet method as previously described³⁸.
335 For MBEC determination, biofilms were allowed to form for 24 hours prior to washing off planktonic
336 cultures with sterile de-ionized water then treatment with CBG at varying concentrations.

337 Quantification of biofilm was performed as noted above.

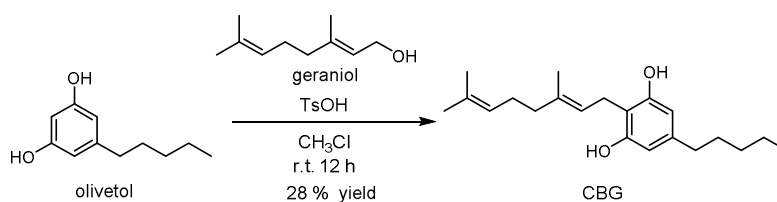
338 **Membrane integrity assays.** DiSC₃(5) assay was performed in *S. aureus* as previously described³⁹. To
339 determine outer membrane and inner membrane activity of CBG against Gram-negative bacteria, we

340 performed β -lactamase and β -galactosidase assays, respectively. Overnight cultures of ML35 pBR322
341 in TSB with 50 $\mu\text{g}/\text{mL}$ ampicillin were 100-fold diluted in fresh pre-warmed TSB and incubated at
342 37°C at 220 rpm. Logarithmic phase cells were collected, washed twice in PBS and then resuspended in
343 PBS at a final OD_{600} of 0.01. Nitrocefin (30 μM) or ONPG (1.5 mM) - probes for β -lactamase and β -
344 galactosidase, respectively (final concentration) - were added to the bacterial suspension and
345 immediately aliquoted to dilution series of CBG and/or PMB at 100 μL final volume. Plates were
346 incubated at 37°C and monitored kinetically for color change at 492 and 405 nm (for nitrocefin and
347 ONPG hydrolysis, respectively). Adequate no drug, no probe and/or cell-free controls were included.
348 **Hemolysis assay.** Hemolysis assay using red blood cells (defibrinated sheep blood, Thermo Fisher
349 Scientific) was performed as previously described⁴⁰.

350 **Statistical analyses.** Statistical analyses were conducted with GraphPad Prism 5.0 and is indicated for
351 each assay in the figure caption. All results are shown as mean \pm SEM unless otherwise stated. In the
352 case of MIC and checkerboard assays, the experiments were repeated at least three independent times
353 and the experiment showing the most conservative effects (if applicable) was shown.

354 Synthesis of Cannabigerol.

355



357

358 CBG was synthesized using a reported procedure⁴¹. To a 25 mL round-bottomed flask containing a
359 magnetic stir were added olivetol (108 mg, 0.6 mmol), chloroform (5 mL), geraniol (174 μL , 1.0
360 mmol), *p*-toluene sulfonic acid monohydrate (19 mg, 0.1 mmol). The flask was covered with aluminum
361 foil and the reaction was stirred at room temperature in the dark for 12 hours at which point TLC
362 analysis indicated complete consumption of the olivetol substrate. To the reaction was added aqueous
363 saturated NaHCO_3 (5 mL). The organic phase was removed and washed with water (5 mL). The
364 aqueous layer was extracted with additional chloroform (5 mL) and the combined organic extracts were
365 dried over MgSO_4 and concentrated *en vacuo*. The crude residue was purified via flash column
366 chromatography on silica gel using gradient elution with hexanes and ethyl acetate. CBG was isolated
367 as an off white powder in 28 % yield (54 mg, 0.17 mmol). Spectral data can be found in Supplementary
368 Figs. 12-14.

369 ¹H NMR (700 MHz, CDCl_3) δ 6.25 (s, 2H), 5.28 (tq, $J = 7.1, 1.3$ Hz, 1H), 5.09 – 5.04 (m, 3H), 3.40 (d,
370 $J = 7.1$ Hz, 2H), 2.49 – 2.43 (m, 2H), 2.14 – 2.04 (m, 4H), 1.82 (s, 3H), 1.68 (s, 3H), 1.60 (s, 3H), 1.58
371 – 1.54 (m, 2H), 1.36 – 1.28 (m, 4H), 0.89 (t, $J = 7.0$ Hz, 3H). ¹³C NMR (176 MHz, CDCl_3) δ 154.92,
372 142.89, 139.13, 132.19, 123.89, 121.84, 110.73, 108.52, 39.83, 35.65, 31.63, 30.93, 26.52, 25.81,
373 22.68, 22.40, 17.83, 16.32, 14.16. HRMS (ESI) m/z : 315.2329 calcd for $\text{C}_{21}\text{H}_{31}\text{O}_2$ [M-H]; 315.24490
obsd.

374 **Mouse infection models.** Animal experiments were conducted according to guidelines set by the
375 Canadian Council on Animal Care using protocols approved by the Animal Review Ethics Board at
376 McMaster University under Animal Use Protocol #17-03-10. Before infection, mice were relocated at
377 random from a housing cage to treatment or control cages. No animals were excluded from analyses,
378 and blinding was considered unnecessary. Seven- to nine-week old female CD-1 mice (Envigo) were
379 infected intraperitoneally with 7.5×10^7 CFU of log-phase MRSA strain USA 300 JE2 with 5% porcine
380 mucin. Treatment of 100 mg/kg CBG or a vehicle solution (60% PEG300 and 5% DMSO) were
381 administered intraperitoneally immediately post-infection. Mice were euthanized and tissues collected
382 into phosphate buffered saline (PBS) at necropsy. Organs were homogenized using a high-throughput

383 tissue homogenizer, serially diluted in PBS, and plated onto solid LB. Plates were incubated overnight
384 at 37°C and colonies were quantified to determine organ load.
385

386 References

- 387 1. WHO *Global priority list of antibiotic-resistant bacteria to guide research, discovery, and*
388 *development of new antibiotics*; World Health Organization: Geneva, 2017.
- 389 2. WHO *Prioritization of pathogens to guide discovery, research and development of new*
390 *antibiotics for drug-resistant bacterial infections including tuberculosis.*; World Health Organization:
391 Geneva, 2017.
- 392 3. Boucher, H. W.; Talbot, G. H.; Bradley, J. S.; Edwards, J. E.; Gilbert, D.; Rice, L. B.; Scheld,
393 M.; Spellberg, B.; Bartlett, J., Bad bugs, no drugs: no ESKAPE! An update from the Infectious
394 Diseases Society of America. *Clin Infect Dis* **2009**, *48* (1), 1-12. DOI: 10.1086/595011.
- 395 4. Nannini, E.; Murray, B. E.; Arias, C. A., Resistance or decreased susceptibility to
396 glycopeptides, daptomycin, and linezolid in methicillin-resistant *Staphylococcus aureus*. *Current*
397 *opinion in pharmacology* **2010**, *10* (5), 516-21. DOI: 10.1016/j.coph.2010.06.006.
- 398 5. Goncalves, J.; Rosado, T.; Soares, S.; Simao, A. Y.; Caramelo, D.; Luis, A.; Fernandez, N.;
399 Barroso, M.; Gallardo, E.; Duarte, A. P., Cannabis and Its Secondary Metabolites: Their Use as
400 Therapeutic Drugs, Toxicological Aspects, and Analytical Determination. *Medicines (Basel)* **2019**, *6*
401 (1). DOI: 10.3390/medicines6010031.
- 402 6. Appendino, G.; Gibbons, S.; Giana, A.; Pagani, A.; Grassi, G.; Stavri, M.; Smith, E.; Rahman,
403 M. M., Antibacterial cannabinoids from *Cannabis sativa*: a structure-activity study. *J Nat Prod* **2008**,
404 *71* (8), 1427-30. DOI: 10.1021/np8002673.
- 405 7. Van Klingeren, B.; Ten Ham, M., Antibacterial activity of delta9-tetrahydrocannabinol and
406 cannabidiol. *Antonie Van Leeuwenhoek* **1976**, *42* (1-2), 9-12.
- 407 8. Turner, C. E.; Elsohly, M. A., Biological activity of cannabichromene, its homologs and
408 isomers. *J Clin Pharmacol* **1981**, *21* (S1), 283S-291S.
- 409 9. Blaskovich, M. A. T.; Kavanagh, A.; Ramu, S.; Levy, S.; Callahan, M.; Thurn, M., Cannabidiol
410 is a Remarkably Active Gram-Positive Antibiotic. In *ASM Microbe Conference*, San Francisco,
411 California, 2019.
- 412 10. Otto, M., Staphylococcal infections: mechanisms of biofilm maturation and detachment as
413 critical determinants of pathogenicity. *Annu Rev Med* **2013**, *64*, 175-88. DOI: 10.1146/annurev-med-
414 042711-140023.
- 415 11. Allison, K. R.; Brynildsen, M. P.; Collins, J. J., Metabolite-enabled eradication of bacterial
416 persisters by aminoglycosides. *Nature* **2011**, *473* (7346), 216-20. DOI: 10.1038/nature10069.
- 417 12. Davies, J.; Davies, D., Origins and evolution of antibiotic resistance. *Microbiol Mol Biol Rev*
418 **2010**, *74* (3), 417-33. DOI: 10.1128/MMBR.00016-10.
- 419 13. Lewis, K., Persister cells, dormancy and infectious disease. *Nat Rev Microbiol* **2007**, *5* (1), 48-
420 56.
- 421 14. Conlon, B. P., *Staphylococcus aureus* chronic and relapsing infections: Evidence of a role for
422 persister cells: An investigation of persister cells, their formation and their role in *S. aureus* disease.
423 *Bioessays* **2014**, *36* (10), 991-6. DOI: 10.1002/bies.201400080.
- 424 15. Lew, D. P.; Waldvogel, F. A., Osteomyelitis. *Lancet* **2004**, *364* (9431), 369-79. DOI:
425 10.1016/S0140-6736(04)16727-5.
- 426 16. Baddour, L. M.; Wilson, W. R.; Bayer, A. S.; Fowler, V. G., Jr.; Tleyjeh, I. M.; Rybak, M. J.;
427 Barsic, B.; Lockhart, P. B.; Gewitz, M. H.; Levison, M. E.; Bolger, A. F.; Steckelberg, J. M.;
428 Baltimore, R. S.; Fink, A. M.; O'Gara, P.; Taubert, K. A., Infective Endocarditis in Adults: Diagnosis,
429 Antimicrobial Therapy, and Management of Complications: A Scientific Statement for Healthcare

- 430 Professionals From the American Heart Association. *Circulation* **2015**, *132* (15), 1435-86. DOI:
431 10.1161/CIR.0000000000000296.
- 432 17. Keren, I.; Kaldalu, N.; Spoering, A.; Wang, Y.; Lewis, K., Persister cells and tolerance to
433 antimicrobials. *FEMS Microbiol Lett* **2004**, *230* (1), 13-8. DOI: S0378109703008565.
- 434 18. Conlon, B. P.; Rowe, S. E.; Gandt, A. B.; Nuxoll, A. S.; Donegan, N. P.; Zalis, E. A.; Clair, G.;
435 Adkins, J. N.; Cheung, A. L.; Lewis, K., Persister formation in *Staphylococcus aureus* is associated
436 with ATP depletion. *Nat Microbiol* **2016**, *1*, 16051. DOI: 10.1038/nmicrobiol.2016.51.
- 437 19. Andre, C. M.; Hausman, J. F.; Guerriero, G., Cannabis sativa: The Plant of the Thousand and
438 One Molecules. *Front Plant Sci* **2016**, *7*, 19. DOI: 10.3389/fpls.2016.00019.
- 439 20. Zheng, X. S.; Chan, T. F.; Zhou, H. H., Genetic and genomic approaches to identify and study
440 the targets of bioactive small molecules. *Chem Biol* **2004**, *11* (5), 609-18. DOI:
441 10.1016/j.chembiol.2003.08.011.
- 442 21. Barker, C. A.; Farha, M. A.; Brown, E. D., Chemical genomic approaches to study model
443 microbes. *Chem Biol* **2010**, *17* (6), 624-32. DOI: 10.1016/j.chembiol.2010.05.010.
- 444 22. Peters, J. M.; Colavin, A.; Shi, H.; Czarny, T. L.; Larson, M. H.; Wong, S.; Hawkins, J. S.; Lu,
445 C. H. S.; Koo, B. M.; Marta, E.; Shiver, A. L.; Whitehead, E. H.; Weissman, J. S.; Brown, E. D.; Qi, L.
446 S.; Huang, K. C.; Gross, C. A., A Comprehensive, CRISPR-based Functional Analysis of Essential
447 Genes in Bacteria. *Cell* **2016**, *165* (6), 1493-1506. DOI: 10.1016/j.cell.2016.05.003.
- 448 23. Fey, P. D.; Endres, J. L.; Yajjala, V. K.; Widhelm, T. J.; Boissy, R. J.; Bose, J. L.; Bayles, K.
449 W., A genetic resource for rapid and comprehensive phenotype screening of nonessential
450 *Staphylococcus aureus* genes. *MBio* **2013**, *4* (1), e00537-12. DOI: 10.1128/mBio.00537-12.
- 451 24. Hurdle, J. G.; O'Neill, A. J.; Chopra, I.; Lee, R. E., Targeting bacterial membrane function: an
452 underexploited mechanism for treating persistent infections. *Nat Rev Microbiol* **2011**, *9* (1), 62-75.
453 DOI: 10.1038/nrmicro2474.
- 454 25. Farha, M. A.; French, S.; Stokes, J. M.; Brown, E. D., Bicarbonate Alters Bacterial
455 Susceptibility to Antibiotics by Targeting the Proton Motive Force. *ACS Infect Dis* **2018**, *4* (3), 382-
456 390. DOI: 10.1021/acscinfedis.7b00194.
- 457 26. Deiana, S.; Watanabe, A.; Yamasaki, Y.; Amada, N.; Arthur, M.; Fleming, S.; Woodcock, H.;
458 Dorward, P.; Pigliacampo, B.; Close, S.; Platt, B.; Riedel, G., Plasma and brain pharmacokinetic profile
459 of cannabidiol (CBD), cannabidivarin (CBDV), Delta(9)-tetrahydrocannabivarin (THCV) and
460 cannabigerol (CBG) in rats and mice following oral and intraperitoneal administration and CBD action
461 on obsessive-compulsive behaviour. *Psychopharmacology (Berl)* **2012**, *219* (3), 859-73. DOI:
462 10.1007/s00213-011-2415-0.
- 463 27. Delcour, A. H., Outer membrane permeability and antibiotic resistance. *Biochim Biophys Acta*
464 **2009**, *1794* (5), 808-16. DOI: 10.1016/j.bbapap.2008.11.005.
- 465 28. Krishnamoorthy, G.; Wolloscheck, D.; Weeks, J. W.; Croft, C.; Rybenkov, V. V.; Zgurskaya,
466 H. I., Breaking the Permeability Barrier of *Escherichia coli* by Controlled Hyperporination of the Outer
467 Membrane. *Antimicrob Agents Chemother* **2016**, *60* (12), 7372-7381. DOI: 10.1128/AAC.01882-16.
- 468 29. Powers, M. J.; Trent, M. S., Expanding the paradigm for the outer membrane: *Acinetobacter*
469 *baumannii* in the absence of endotoxin. *Mol Microbiol* **2018**, *107* (1), 47-56. DOI: 10.1111/mmi.13872.
- 470 30. Lehrer, R. I.; Barton, A.; Ganz, T., Concurrent assessment of inner and outer membrane
471 permeabilization and bacteriolysis in *E. coli* by multiple-wavelength spectrophotometry. *J Immunol*
472 *Methods* **1988**, *108* (1-2), 153-8.
- 473 31. Worthington, R. J.; Melander, C., Combination approaches to combat multidrug-resistant
474 bacteria. *Trends Biotechnol* **2013**, *31* (3), 177-84. DOI: 10.1016/j.tibtech.2012.12.006.
- 475 32. Stokes, J. M.; MacNair, C. R.; Ilyas, B.; French, S.; Cote, J. P.; Bouwman, C.; Farha, M. A.;
476 Sieron, A. O.; Whitfield, C.; Coombes, B. K.; Brown, E. D., Pentamidine sensitizes Gram-negative
477 pathogens to antibiotics and overcomes acquired colistin resistance. *Nat Microbiol* **2017**, *2*, 17028.
478 DOI: 10.1038/nmicrobiol.2017.28.

- 479 33. CLSI, *Methods for Dilution Antimicrobial Susceptibility Tests for Bacteria That Grow*
480 *Aerobically; Approved Standard—Ninth Edition*. CLSI document M07-A9. Clinical and Laboratory
481 Standards Institute: Wayne, PA, 2012.
- 482 34. Vaara, M.; Porro, M., Group of peptides that act synergistically with hydrophobic antibiotics
483 against gram-negative enteric bacteria. *Antimicrob. Agents Chemother.* **1996**, *40* (8), 1801-1805.
- 484 35. Kim, W.; Zhu, W.; Hendricks, G. L.; Van Tyne, D.; Steele, A. D.; Keohane, C. E.; Fricke, N.;
485 Conery, A. L.; Shen, S.; Pan, W.; Lee, K.; Rajamuthiah, R.; Fuchs, B. B.; Vlahovska, P. M.; Wuest, W.
486 M.; Gilmore, M. S.; Gao, H.; Ausubel, F. M.; Mylonakis, E., A new class of synthetic retinoid
487 antibiotics effective against bacterial persisters. *Nature* **2018**, *556* (7699), 103-107. DOI:
488 10.1038/nature26157.
- 489 36. Caspi, R.; Billington, R.; Fulcher, C. A.; Keseler, I. M.; Kothari, A.; Krummenacker, M.;
490 Latendresse, M.; Midford, P. E.; Ong, Q.; Ong, W. K.; Paley, S.; Subhraveti, P.; Karp, P. D., The
491 MetaCyc database of metabolic pathways and enzymes. *Nucleic Acids Res* **2018**, *46* (D1), D633-D639.
492 DOI: 10.1093/nar/gkx935.
- 493 37. Sambrook, J.; Fritsch, E. F.; Maniatis, T., *Molecular cloning: a laboratory manual*. 2nd ed.;
494 Cold Spring Harbor Laboratory: Cold Spring Harbor, New York, 1990.
- 495 38. Merritt, J. H.; Kadouri, D. E.; O'Toole, G. A., Growing and analyzing static biofilms. *Curr*
496 *Protoc Microbiol* **2005**, *Chapter 1*, Unit 1B 1. DOI: 10.1002/9780471729259.mc01b01s00.
- 497 39. Farha, M. A.; Verschoor, C. P.; Bowdish, D.; Brown, E. D., Collapsing the proton motive force
498 to identify synergistic combinations against *Staphylococcus aureus*. *Chem Biol* **2013**, *20* (9), 1168-78.
499 DOI: 10.1016/j.chembiol.2013.07.006.
- 500 40. Barker, W. T.; Chandler, C. E.; Melander, R. J.; Ernst, R. K.; Melander, C., Tryptamine
501 derivatives disarm colistin resistance in polymyxin-resistant gram-negative bacteria. *Bioorg Med Chem*
502 **2019**, *27* (9), 1776-1788. DOI: 10.1016/j.bmc.2019.03.019.
- 503 41. Taura, F.; Morimoto, S.; Shoyama, Y., Purification and characterization of cannabidiolic-acid
504 synthase from *Cannabis sativa* L.. Biochemical analysis of a novel enzyme that catalyzes the
505 oxidocyclization of cannabigerolic acid to cannabidiolic acid. *J Biol Chem* **1996**, *271* (29), 17411-6.
506 DOI: 10.1074/jbc.271.29.17411.

507

508

509

510

511

512

513

514

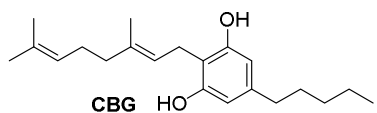
515

516

517

518

519 Table 1. Physicochemical properties of CBG as calculated by ACD/Percepta software.



Phys Chem Profile		Lead-like?
MW	316.48	good
Log P	6.74	very lipophilic
H-Donors	2	good
H-Acceptors	2	good
Rotatable Bonds	9	good
Rings	1	good
Predicted solubility	0.0003 mg/mL	highly insoluble

520

521

522

523

524

525

526

527

528

529

530

531

532

533

534

535

536

537

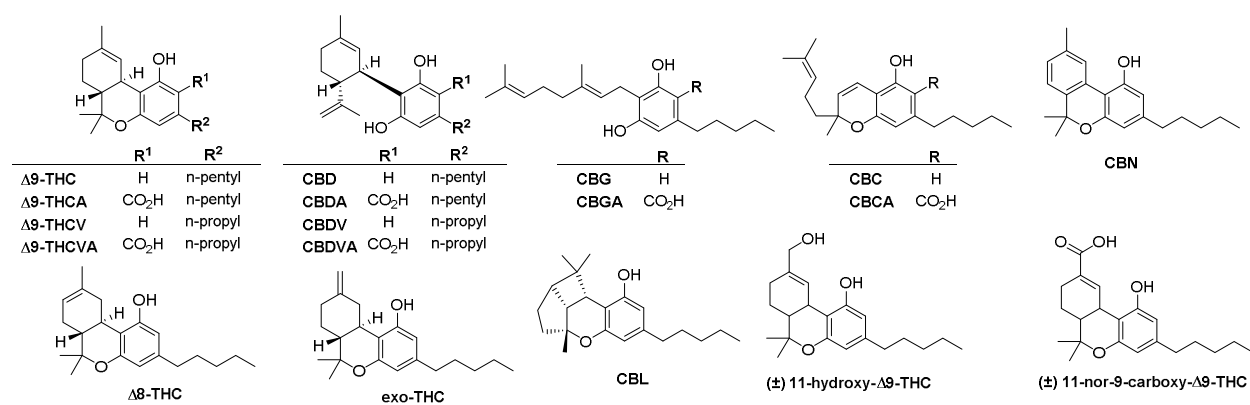
538

539

540

541

542



543

544

545 Fig. 1. Structures of the cannabinoids surveyed in this study.

546

547

548

549

550

551

552

553

554

555

556

557

558

559

560

561

562

563

564

565

566

567

568

569

570

571

572

573

574

575

576

577

578

579

580

581

582

583

584

585

586

587

588

589

590

591

592

593

594

595

596

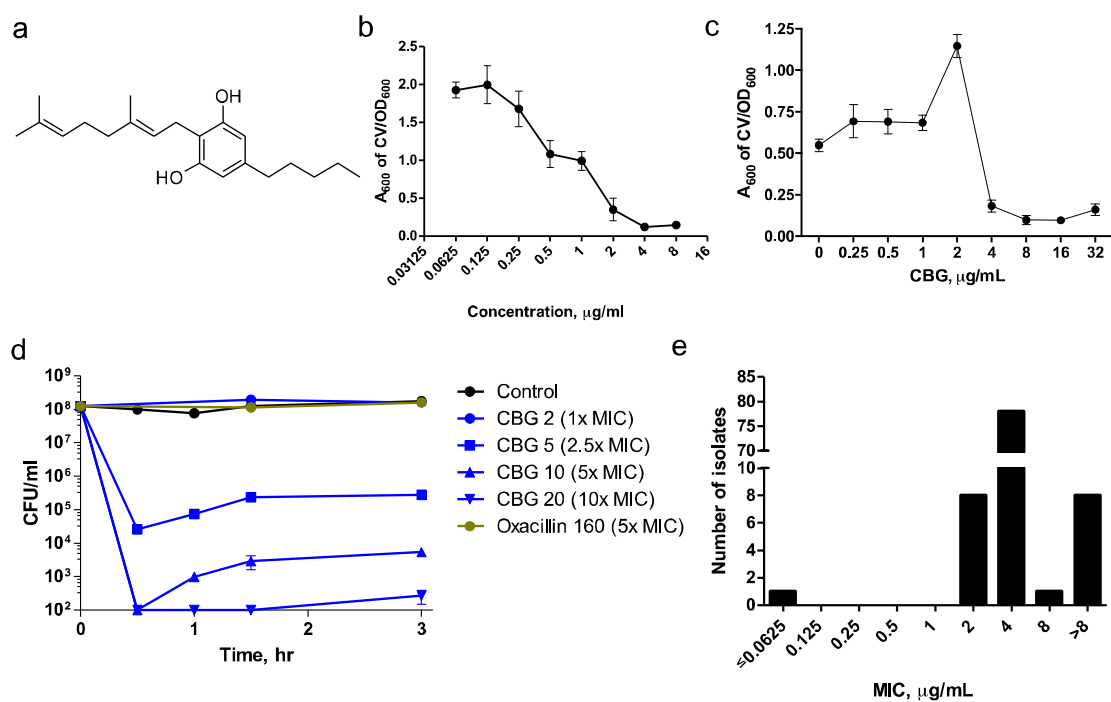


Fig. 2. Cannabigerol (CBG) is a potent antibacterial, anti-biofilm and anti-persister cannabinoid. **a**, Chemical structure of CBG **b**, Concentration dependence for inhibition of MRSA biofilm formation by CBG. Shown is the average A_{600nm} measurements of crystal violet stained biofilms and normalized by the OD₆₀₀ of planktonic cells with error bars representing one standard error of the mean, S.E.M. ($n=4$). **c**, Minimum biofilm eradication concentration of CBG. CBG is capable of eradicating pre-formed biofilms at a concentration of 4 μg/mL ($n=8$). **d**, Time-kill curve of *S. aureus* USA300 persisters by CBG compared to oxacillin shown as mean \pm S.E.M ($n=4$). CBG rapidly eradicated a population of $\sim 10^8$ CFU/ml MRSA persisters to below the detection threshold within 30 minutes of treatment. On the other hand, the β -lactam oxacillin at 160 μg/mL (5x MIC) did not show any activity against the same population of persisters. **e**, MIC₉₀ distribution of CBG against clinical isolates of MRSA ($n=96$). The MIC₉₀ is 4 μg/mL.

597

598

599

600

601

602

603

604

605

606

607

608

609

610

611

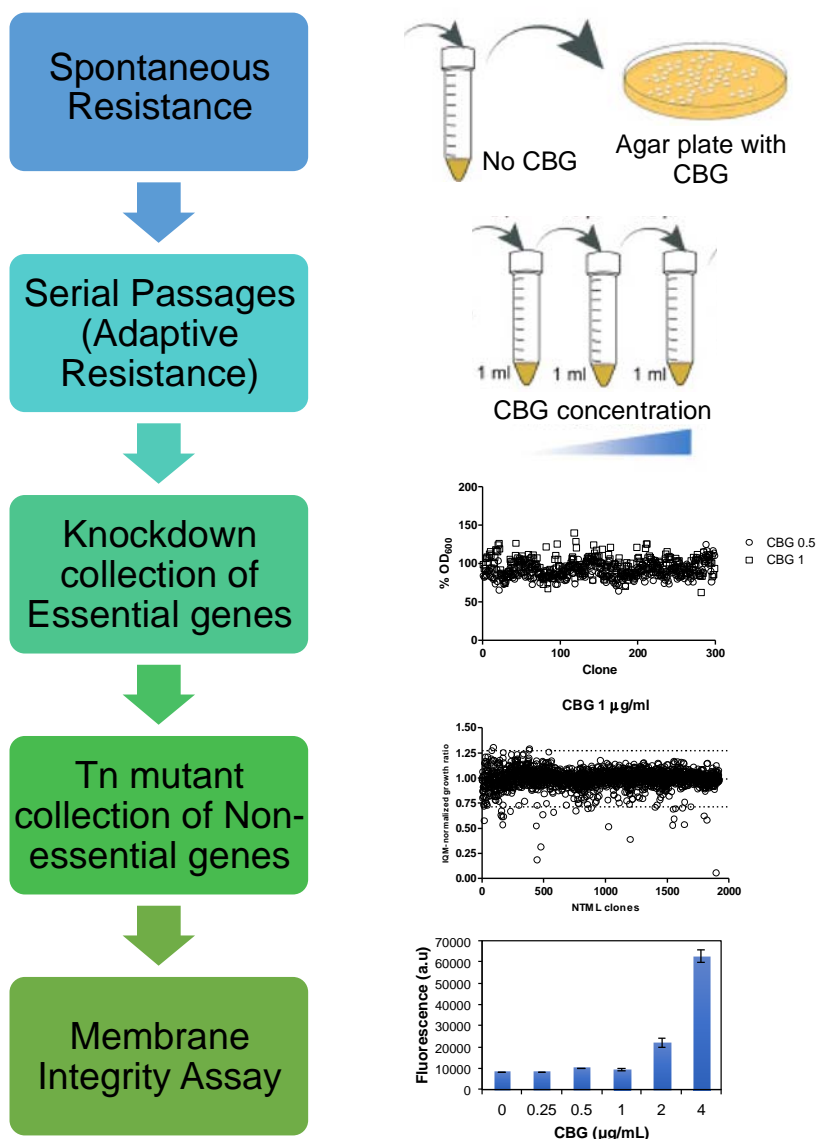
612

613

614

615

616



617 **Fig. 3.** CBG is active on the cytoplasmic membrane of MRSA. Overview of strategies for mechanism of action
618 determination, culminating in the finding that CBG is active on the cytoplasmic membrane, as determined by
619 dose-dependent increases in DiSC₃(5) fluorescence.

620

621

622

623

624

625

626
627
628
629
630
631
632
633
634
635
636
637
638
639
640
641
642
643
644
645
646
647
648
649
650
651
652
653
654
655

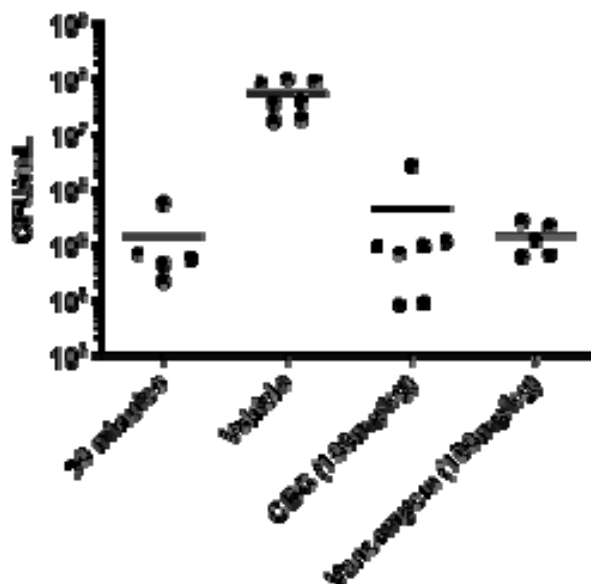


Fig. 4. CBG is efficacious in a systemic mouse model of *S. aureus* infection. A single-dose treatment is administered immediately post-infection: vehicle control (n=7, i.p.), CBG (n=7, 100 mg kg⁻¹, i.p.) or vancomycin control (n=5, 100 mg kg⁻¹, i.p.). Colony-forming units (CFU) within spleen tissue were enumerated at 7 h post-infection. CFUs within spleen tissue were also enumerated at an early time point of 30 minutes post-infection following vehicle control treatment (n=5, i.p.). Horizontal lines represent the geometric mean of the bacterial load for each treatment group. Administration of CBG resulted in a 2.8-log₁₀ reduction ($p < 0.001$, Mann–Whitney *U*-test) in CFU when compared to the vehicle control.

656

657

658

659

660

661

662

663

664

665

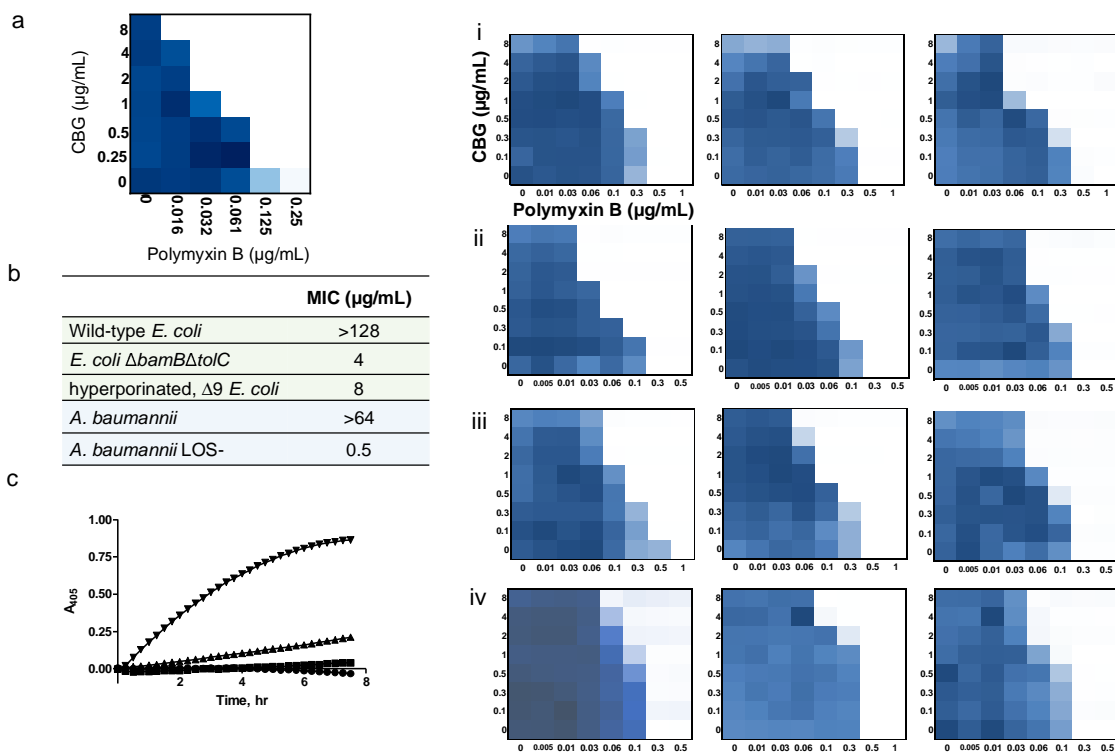
666

667

668

669

670



671

672

673

674

675

676

677

678

679

680

681

682

683

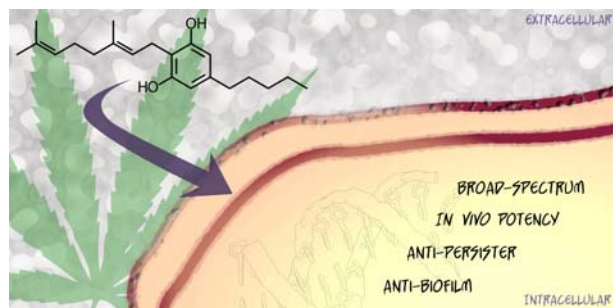
684

685

686

Fig. 5. CBG is active against Gram-negative bacteria whose outer membrane is permeabilized, where it acts on the inner membrane. **a**, Checkerboard analysis of CBG in combination with polymyxin B against *E. coli*. The extent of inhibition is shown as a heat plot, such that the darkest blue color represents full bacterial growth. **b**, CBG becomes active against Gram-negative bacteria in various genetic backgrounds where the outer membrane is compromised. **c**, CBG acts on the IM of *E. coli* but only in the presence of sub-lethal concentration of polymyxin B (PmB), unmasking cytoplasmic β -galactosidase leading to hydrolysis of ONPG as detected via absorbance reads at 405 nm over time. Conditions were as follows: control (circles), CBG 2 $\mu\text{g/mL}$ (squares), PmB 0.125 $\mu\text{g/mL}$ (triangles) and PmB 0.125 $\mu\text{g/mL}$ + CBG 2 $\mu\text{g/mL}$ (inverted triangles). **d**, CBG in combination with polymyxin B against multi-drug resistant clinical isolates of i, *A. baumannii*, ii, *E. coli*, iii, *K. pneumoniae*, iv, *P. aeruginosa*. The extent of inhibition is shown as a heat plot, such that the darkest blue color represents full bacterial growth.

687 For Table of Contents Use Only



688